J. Am. Soc. Mass Spectrom. (2012) 23:889–898
DOI: 10.1007/s13361-012-0342-x

RESEARCH ARTICLE

Validation of Membrane Protein Topology Models by Oxidative Labeling and Mass Spectrometry

Yan Pan,[1] Xiang Ruan,[2] Miguel A. Valvano,[2] Lars Konermann[1]

[1]Department of Chemistry, The University of Western Ontario, London, Ontario, N6A 5B7, Canada
[2]Center for Human Immunology, Departments of Microbiology and Immunology, and Medicine, The University of Western Ontario, London, N6A 5C1, Canada

Abstract

Computer-assisted topology predictions are widely used to build low-resolution structural models of integral membrane proteins (IMPs). Experimental validation of these models by traditional methods is labor intensive and requires modifications that might alter the IMP native conformation. This work employs oxidative labeling coupled with mass spectrometry (MS) as a validation tool for computer-generated topology models. ·OH exposure introduces oxidative modifications in solvent-accessible regions, whereas buried segments (e.g., transmembrane helices) are non-oxidizable. The *Escherichia coli* protein WaaL (O-antigen ligase) is predicted to have 12 transmembrane helices and a large extramembrane domain (Pérez et al., Mol. Microbiol. **2008,** *70*, 1424). Tryptic digestion and LC-MS/MS were used to map the oxidative labeling behavior of WaaL. Met and Cys exhibit high intrinsic reactivities with ·OH, making them sensitive probes for solvent accessibility assays. Overall, the oxidation pattern of these residues is consistent with the originally proposed WaaL topology. One residue (M151), however, undergoes partial oxidation despite being predicted to reside within a transmembrane helix. Using an improved computer algorithm, a slightly modified topology model was generated that places M151 closer to the membrane interface. On the basis of the labeling data, it is concluded that the refined model more accurately reflects the actual topology of WaaL. We propose that the combination of oxidative labeling and MS represents a useful strategy for assessing the accuracy of IMP topology predictions, supplementing data obtained in traditional biochemical assays. In the future, it might be possible to incorporate oxidative labeling data directly as constraints in topology prediction algorithms.

Key words: Membrane protein, Methionine oxidation, Electrospray ionization, Lipopolysaccharide, O-antigen ligase, Protein structure

Introduction

Integral membrane proteins (IMPs) play an essential role in numerous biological processes. In addition, IMPs are important drug targets [1, 2]. Yet, the understanding of IMP structure and function is limited compared with the vast amount of information available for water-soluble proteins [3]. IMPs possess a largely nonpolar exterior that interacts with acyl chains of the membrane bilayer. Most IMPs are α-helix bundles. They contain hydrophobic (or amphipathic) transmembrane helices that are linked by hydrophilic loops, which protrude into the aqueous environment [4]. Due to their nonpolar character, IMPs are prone to aggregation in solution. Solubilization in detergents such as dodecyl-β-D-maltoside (DM) is required for structural/functional studies on native IMPs outside their natural lipid bilayer environment [5].

The difficulties associated with X-ray or NMR structural investigations [3] have spurred the development of low-resolution

Correspondence to: Lars Konermann; *e-mail:* konerman@uwo.ca

Received: 14 December 2011
Revised: 12 January 2012
Accepted: 17 January 2012
Published online: 13 March 2012

approaches for predicting IMP topologies (i.e., the location of helices and loops, and the protein orientation relative to the cytoplasm [6]). Kyte and Doolittle hydropathy analyses represent a widely used strategy. In this approach transmembrane helices are tentatively identified as sequence regions of ~19 hydrophobic residues that are separated by hydrophilic stretches (loops) [7]. Prediction algorithms of this type have been refined in recent years by allowing the incorporation of homology information and various constraints [4, 8, 9]. Nonetheless, even these advanced computational tools can generate misleading topology predictions [10]. Experimental validation of the resulting models, therefore, is absolutely essential.

Substituted cysteine accessibility methods (SCAM [10]) represent a key approach for the validation of topology models. Only thiol groups located in solvent-accessible regions react with -SH specific labeling agents. The extent of labeling can be monitored using fluorescence methods. SCAM requires a cysteine-free background construct, and a large number of single site mutants [10, 11]. Protease accessibility assays coupled with gel electrophoresis represent another possible method [12, 13]. In addition, truncated IMP variants can be expressed as fusion proteins. Colorimetric assays or fluorescence techniques can then report on the location of the fused moiety (i.e., cytoplasmic versus extracellular (or periplasmic) [6, 13–16]). A drawback of these traditional biochemical methods is their labor intensive nature. More importantly, any sequence alterations may disrupt the native protein fold [10].

Mass spectrometry (MS) is increasingly being used for various types of IMP studies [1, 17–28]. Covalent labeling coupled with MS [29] can provide structural information on IMPs. Protein exposure to a hydrophilic reactive probe induces covalent modifications in solvent-accessible regions, whereas buried segments are sterically protected from the labeling agent [30]. The location(s) and the extent of labeling can be determined by LC-MS/MS peptide mapping [31, 32]. Such experiments have been used to explore conformational features and interactions of IMPs [32–42]. For IMP topology studies, however, this approach remains underutilized.

Hydroxyl radical (·OH) is a widely used covalent labeling agent that can be produced in various ways [31, 35, 43–47]. A simple strategy is the photolysis of dilute H_2O_2 by a pulsed UV laser [48, 49]. This laser-induced oxidative labeling approach is sometimes referred to as fast photochemical oxidation of proteins (FPOP) [50]. Under single-exposure conditions, this technique is free of labeling-induced structural artifacts [50, 51]. Oxidative modifications typically appear as +16 Da adducts, although other mass shifts can occur as well [31]. The extent of modification at any given side chain depends on a combination of solvent-accessibility and intrinsic reactivity [52]. The presence of sulfur in Cys and Met makes these two amino acids by far the most reactive [53]. For IMPs it is not uncommon to observe hydroxyl radical-induced modifications almost exclusively at these sulfur-containing residues [33, 54, 55]. Our laboratory has recently applied laser-induced oxidative labeling for mapping conformational transitions of bacteriorhodopsin, an IMP with a well known three-dimensional structure [42]. In the current work, we extend this approach to probe the topology of an IMP for which no high-resolution structural information is available.

Lipopolysaccharide (LPS) is a major component of the outer membrane of gram-negative bacteria [56]. LPS consists of lipid A, core oligosaccharide, and O antigen [57]. The O antigen is synthesized as a lipid-linked glycan intermediate, and it is ligated to the lipid A-core oligosaccharide prior to export of the complete LPS molecule to the bacterial surface [58]. WaaL is an inner membrane IMP that catalyzes this ligation [13, 15, 59]. Application of the prediction algorithm TMHHM [60] in combination with biochemical assays yielded a topology model of *E. coli* WaaL that involves 12 transmembrane helices (Figure 1 [13]). Both termini are located on the cytoplasmic side. Molecular modeling suggests that the large extramembrane domain EL5 connecting the putative helices 9 and 10 adopts a tightly folded globular structure [13].

This study employs laser-induced oxidative labeling and MS to validate the existing WaaL topology model [13]. The resulting data support many features of the original prediction. Nonetheless, it is found that a slightly revised WaaL topology is in better agreement with the observed oxidation behavior than the original model.

Experimental

Materials and Sample Preparation

Sodium phosphate, DM, ammonium bicarbonate, and formic acid were purchased from Sigma (St. Louis, MO, USA). Sequencing-grade modified trypsin was purchased from Promega (Madison, WI, USA). RapiGest SF is an acid-labile surfactant that was obtained from Waters (Milford, MA, USA). All chemicals were used as received. Wild-type WaaL consists of 419 amino acids. The experiments of this work were carried out on a WaaL construct with a C-terminal FLAG-His10x tag, containing 32 additional residues, and resulting in an overall average MW of 50794.8 Da. The protein was purified from *E. coli* JM105v by Ni^{2+}-affinity chromatography, and it was subsequently concentrated using a 30 kDa cutoff membrane as described [59]. This method afforded ~1 mg of WaaL protein per liter of culture. The experiments of this study were conducted on DM-solubilized protein. Enzyme activity was verified by an in vitro ligation assay [59]. Buffer exchange yielded stock solutions containing 100 μM WaaL, 0.05% (wt/vol) DM, 150 mM sodium chloride, 12.5 mM imidazole, 10% glycerol, and 50 mM sodium phosphate (pH 8).

Oxidative Labeling

Pulsed ·OH labeling was performed using a two-syringe continuous-flow device similar to that described previously [61]. Syringe 1 contained 20 μM WaaL in 0.05 % DM and

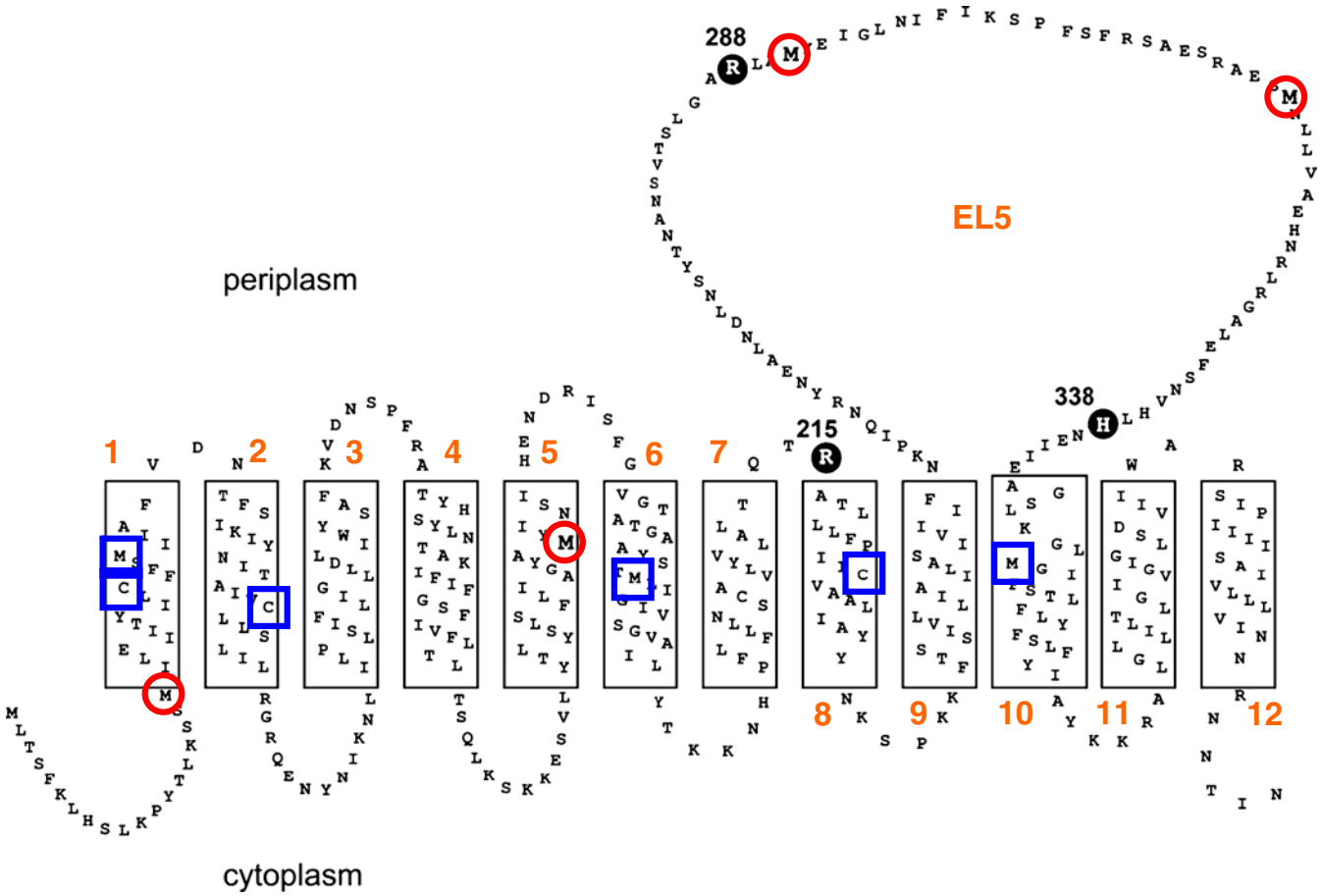

Figure 1. Topology of WaaL predicted by TMHMM [60] (modified from Pérez et al. [13]). Transmembrane helices 1, 2, … are denoted as rectangles. A large external domain is denoted as EL5. Residues that undergo oxidative labeling are highlighted using red circles, whereas blue squares indicate Cys/Met residues that are protected from oxidation (see later, Figure 4). One Met and one Cys were not covered by peptide mapping (not highlighted in this Figure). Three conserved residues involved in enzyme function (R215, R288, and H338) [13] are marked in black. The topology map was displayed using VHMTP [66]

150 mM NaCl, 2.5 mM imidazole, 50 mM phosphate buffer (pH 8), 2% glycerol, and 30 mM glutamine, while syringe 2 contained 0.3% (vol/vol) H_2O_2 and 0.05% DM in phosphate buffer (pH 8). Both syringes were advanced simultaneously at 20 µL min^{-1} using a syringe pump (Harvard Apparatus, Boston, MA,, USA). A KrF excimer laser (EX 50IN; GAM Laser, Orlando, FL, USA) producing 18 ns pulses at 248 nm, 32 Hz, and 37 mJ $pulse^{-1}$ was used to generate hydroxyl radicals by H_2O_2 photolysis within the reaction capillary made of a 100 µm i.d. fused silica. The beam diameter at the irradiation point was around 1 mm. Glutamine acts as a radical scavenger that quenches the labeling reaction on the time scale of 1 µs [48].

Capillary outflow aliquots of ~120 µL were collected in microcentrifuge tubes containing 10 µL of 200 mM methionine and 10 µL 2 µM catalase (pH 7) for deactivating residual H_2O_2 and other oxidizing agents that otherwise might contribute to undesired "secondary" oxidation [62–65]. All samples were lyophilized and subsequently redissolved in 60 µL of 100 mM ammonium bicarbonate buffer (pH 8) containing 0.2% (wt/vol) RapiGest. The resulting solutions were digested with trypsin for 24 h at 37 °C using a 1:10 (wt/wt) enzyme:protein ratio. Tryptic peptides were analyzed by UPLC/ESI-MS employing a C18 BEH 130 column (2.1×100 mm, particle size 1.7 µm, Waters) and a Waters Q-TOF Ultima mass spectrometer. For each injection, 8 µL of digested sample were loaded onto the UPLC column without surfactant removal. Chromatographic separations were carried out at 40 °C and at a flow rate of 80 µL min^{-1}. Solvent A was 0.1% aqueous formic acid, and solvent B consisted of 50:50 (vol/vol) acetonitrile/isopropanol with 0.1% formic acid. Elution started with isocratic flow (4 min, 2% B for desalting), followed by a 50 min linear gradient from 15% to 90% B in 50 min for peptide separation. After each run, 20 µL of formic acid were injected onto the column, and the column was washed with 90% B for 30 min. Confirmation of peptide identities and localization of oxidation sites was performed by collision-induced dissociation (CID) tandem MS conducted in data-dependent acquisition mode. The resulting MS/MS data were analyzed

manually using the MassLynx software package supplied by the instrument manufacturer.

Data Analysis

The extent of oxidation for each peptide is reported as "fraction unmodified," F_u, defined as

$$F_u = A_u/(A_u + A_{ox}) \quad (1)$$

where A_u and A_{ox} are the integrated MS peak areas of the unmodified species and its oxidation products, respectively [31]. The application of this equation rests on the assumption that unmodified peptides and their corresponding oxidation products exhibit similar ionization efficiencies. Previous studies have confirmed that this assumption is justified for the types of modifications discussed here [31, 44]. Fortuitously, none of the WaaL tryptic peptides was found to contain more than one oxidized residue (as discussed below). Hence, the peptide F_u values reported in this work directly reflect the oxidation behavior of individual residues.

Even in the absence of laser exposure, the protein exhibits a low amount of background oxidation. This effect can be caused by the presence of H_2O_2 in the reaction mixture, but some oxidation may also occur during sample handling and storage [62–65]. Following procedures established previously [54], all F_u values were therefore subjected to background correction according to

$$F_u = \frac{F_u^{app}}{F_u^{bgr}} \quad (2)$$

where F_u^{app} is the "apparent" fraction unmodified, obtained by applying eq 1 directly to data acquired after labeling. F_u^{bgr} represents the fraction unmodified for non-irradiated control samples. F_u values reported below represent an average of three independent measurements, each with its own background correction. Error bars reflect the maximum deviation from the average value.

Results and Discussion

Oxidative Labeling of WaaL

Laser-induced oxidative labeling of DM-solubilized WaaL results in several +16 Da modifications. Using manual inspection of the experimental data, we did not find evidence for reaction products associated with any other mass shifts. Tryptic peptide mapping was employed to identify oxidation sites. UPLC/MS allowed the detection of 21 tryptic peptides, corresponding to ~93% sequence coverage (Table 1). Significant oxidative labeling was found only for four peptides: T3-5, T13, T22, and T25. Oxidation of these protein segments is evident from intense +16 Da signals in the spectra of the laser-irradiated samples (Figure 2b, d, j, and l). These oxidation signals are virtually absent in the spectra of the non-irradiated controls (Figure 2a, c, i, and k). All other peptides show mass distributions that are virtually indistinguishable before and after ·OH exposure. Figure 2 exemplifies this lack of oxidative labeling for T14-15 (Figure 2e, f), T17-18 (Figure 2g, h), and T28 (Figure 2m, n). Each of the peptides included in Figure 2 contains at least one highly reactive sulfur-containing residue (Cys or Met). Unfortunately, residues M1 and C203 were not covered by our mapping approach because the corresponding peptides (T1 and T16) were not detectable under the conditions used here (Table 1).

The four oxidized peptides (T3-5, T13, T22, and T25) were subjected to MS/MS for pinpointing the exact locations of modification sites. Figure 3 shows partial tandem mass spectra of T3-5 for a non-irradiated control (panel a), and T3-5 +16

Table 1. Identified Tryptic Peptides of WaaL. Methionine and Cysteine Residues are Underlined. T2, T6, *etc*. Denotes the Peptide Location Within the WaaL Sequence, Numbers in Brackets Represent the Amino Acid Range. Species such as T3-5 Represent Peptides with Missed Cleavages. Peptides T1 (1-6) MLTSFK, and T16 (193-215) NHPFLFLLNSCAVLYVLALTQTR were not Detected

Peptide	Sequence	Mass (Da)	*m/z*
T2 (7-16)	LHSLKPYTLK	1198.71	600.36
T3-5 (17-63)	SSMILEIITYILCFFSMIIAFVDNTFSIKIYNITAIVCLLSLILRGR	5370.93	1343.74
T6 (64-70)	QENYNIK	907.44	454.73
T7 (71-93)	NLILPLSIFLIGLLDLIWYSAFK	2662.55	1331.79
T8 (94-100)	VDNSPFR	833.40	417.71
T9-10 (101-129)	ATYHSYLNTAKIFIFGSFIVFLTLTSQLK	3322.80	1108.61
T9-11 (101-131)	ATYHSYLNTAKIFIFGSFIVFLTLTSQLKSK	3537.93	885.49
T12-13 (132-161)	KESVLYTLYSLSFLIAGYAMYINSIHENDR	3509.75	1170.93
T13 (133-161)	ESVLYTLYSLSFLIAGYAMYINSIHENDR	3381.66	1128.33
T14-15 (162-192)	ISFGVGTATGAAYSTMLIGIVSGVAILYTKK	3088.69	1030.57
T17-18 (216-238)	ATLLLFPIICVAALIAYYNKSPK	2521.44	841.49
T19-20 (239-265)	KFTSSIVLLIAILASIVIIFNKPIQNR	3010.83	1004.62
T21 (266-288)	YNEALNDLNSYTNANSVTSLGAR	2486.17	1244.09
T22 (289-301)	LAMYEIGLNIFIK	1523.84	762.93
T21-23 (266-307)	YNEALNDLNSYTNANSVTSLGARLAMYEIGLNIFIKSPFSFR	4713.35	1179.35
T25 (313-325)	AESMNLLVAEHNR	1482.72	742.37
T24-26 (308-327)	SAESRAESMNLLVAEHNRLR	2282.15	761.73
T27 (328-348)	GALEFSNVHLHNEIIEAGSLK	2277.18	760.07
T28 (349-369)	GLMGIFSTLFLYFSLFYIAYK	2493.31	1247.66
T32 (396-414)	SIPIIIISAIVLLLVINNR	2073.33	1037.67
T31-32 (372-414)	ALGLLILTLGIVGIGLSDVIIWARSIPIIIISAIVLLLVINNR	4530.84	1133.72

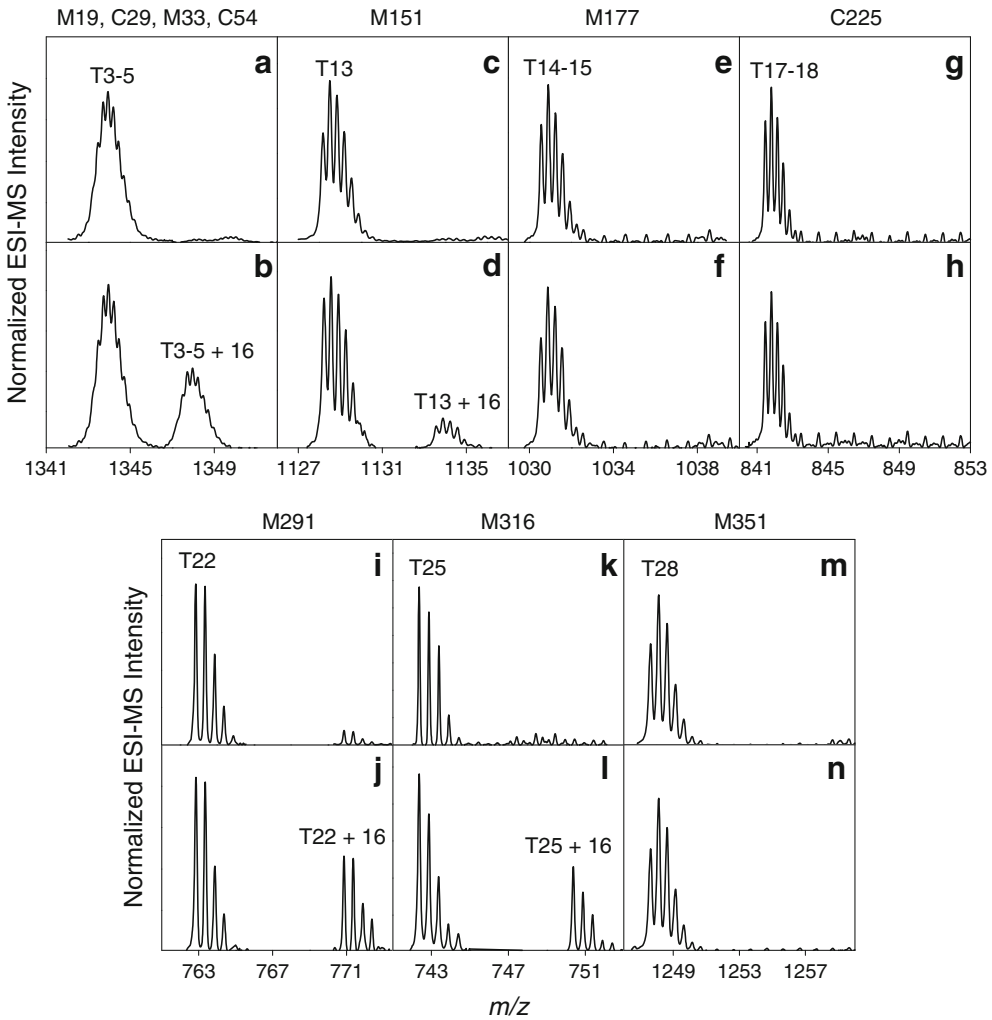

Figure 2. Illustrative UPLC/ESI mass spectra of tryptic WaaL peptides that contain potential oxidation sites (Met and Cys). The panels are arranged in pairs (a/b, c/d, etc.), depicting data for unlabeled control samples and for oxidatively labeled WaaL, respectively. Potential oxidation sites are indicated along the top. Oxidized peptides are denoted as "+ 16"

after oxidative labeling (panel b). In both spectra b_2 ions appear at their expected *m/z* ratios. Starting from b_3, the signals originating from the oxidized sample are shifted by 16 Da. This observation identifies M19 as the site of oxidation in T3-5+16. The absence of unmodified b_n ions with $n>2$ in the MS/MS data of Figure 3b reveals that M19 is the *only* oxidized residue in T3-5+16. This finding is notable, because there are three additional highly reactive residues in this peptide (C29, M33, and C54). The lack of oxidation at these three other residues implies that they are not solvent-accessible. MS/MS experiments on the peptide T25 (Figure 3c, d) reveal that C-terminal fragment ions up to y_9 appear at the same *m/z* values before and after oxidative labeling. The same is true for b_3, whereas b_4 exhibits a 16 Da shift for the labeled sample. The oxidation site in T25 +16 can therefore be identified as M316 (Figure 3c, d). Similar MS/MS experiments were conducted for T13 and T22. In addition to M19 and M316, those measurements identified M151 and M291 as being oxidized after ·OH exposure of WaaL (data not shown).

The results discussed so far reveal that laser-induced ·OH labeling of WaaL results in four detectable oxidative modifications. All of these correspond to +16 Da mass shifts at Met residues, attributable to methionine sulfoxide (MetO) formation [31]. Oxidation of these residues reveals that they are solvent-accessible. In contrast, methionines M33, M177, M351 are not oxidized and hence not solvent-accessible. Cysteine is known to have an intrinsic ·OH reactivity that is even higher than that of methionine [53]. Cys oxidation should give rise to mass shifts of +32 Da (sulfinic acid) or +48 Da (sulfonic acid) [31, 55], and possibly other oxidation products such as sulfenic acid (+16 Da). Yet, none of the cysteines we mapped were oxidized, implying that C29, C54, and C225 are not solvent-accessible. Consistent with their lower intrinsic reactivities [53], none of the other 18 types of residues were found to be oxidizable under the conditions of our work. This chemical selectivity is reminiscent of data previously obtained for other membrane proteins [33, 54, 55]. The effect is likely caused by the presence of surfactants and other additives that act as ·OH

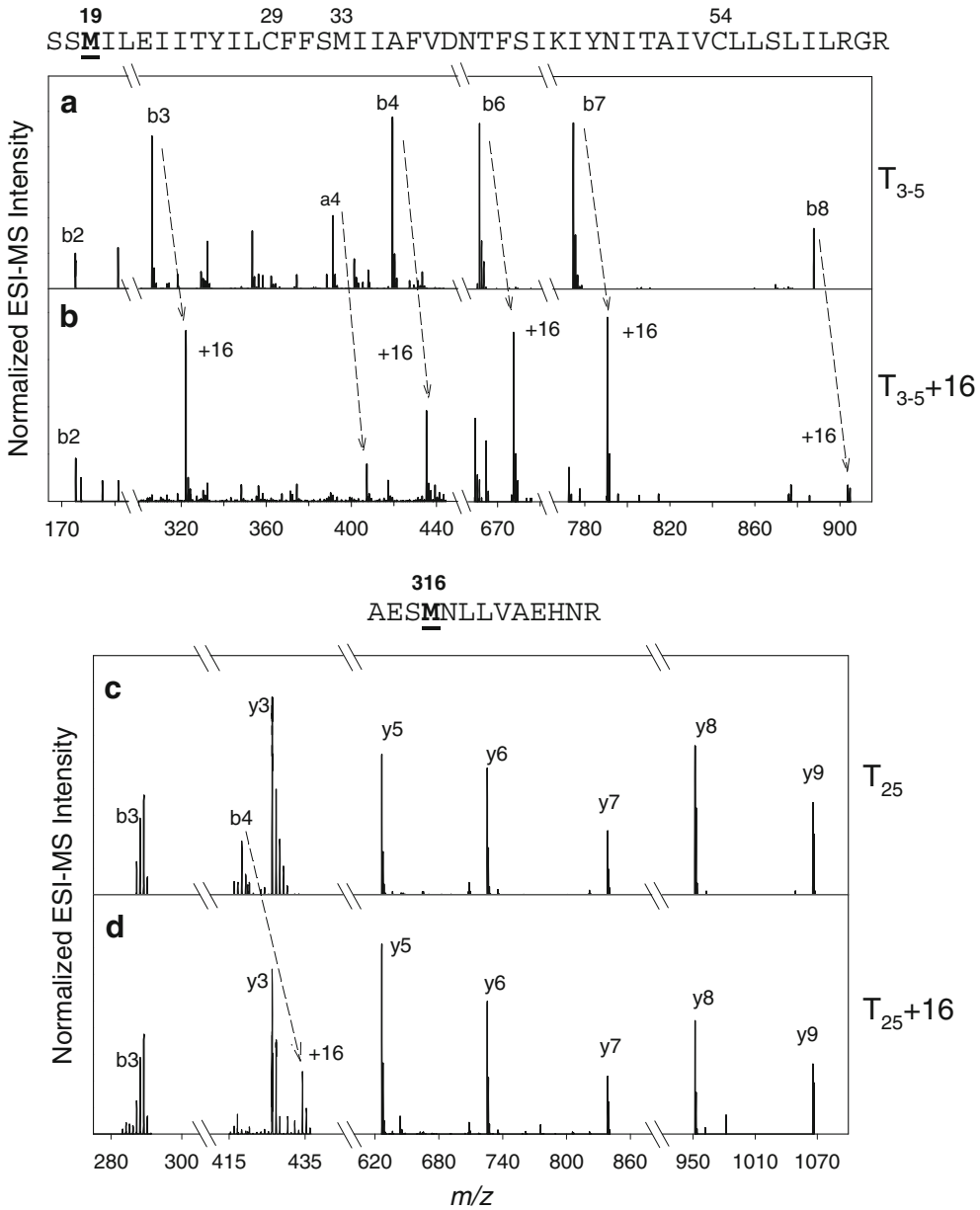

Figure 3. Partial MS/MS spectra of tryptic peptide T3-5 from unlabeled WaaL (precursor *m/z* 1343.74, (**a**), and for the peptide T3-5 +16 after laser-induced oxidative labeling (precursor *m/z* 1347.74, (**b**). These MS/MS data identify M19 as the only oxidation site in this peptide. Also shown (along the top) is the amino acid sequence of T3-5. Similarly, the bottom two panels illustrate the MS/MS behavior of T25 from an unlabeled sample [precursor *m/z* 1482.72, (**c**)] and for oxidatively labeled WaaL [precursor *m/z* 1490.72, (**d**)]. These data reveal that M316 is the only oxidation site in T25+16

scavengers and that outcompete less reactive oxidation pathways. As a result, any oxidation at non-sulfur residues is suppressed [48, 54].

Quantitative Analysis of Oxidation Levels

To quantitatively express the extent of oxidative labeling, we calculated F_u (fraction unmodified) values as outlined in equation 2 [31]. Cys or Met residues that do not undergo oxidation are characterized by $F_u \approx 1$, reflecting a lack of solvent access. In contrast, solvent-accessible reactive side chains show significantly lower F_u values. Roughly 35% of the protein molecules in the reaction mixture undergo hydroxyl radical exposure for the conditions used here [51]. This implies that F_u values around $(1 - 0.35) = 0.65$ are expected for residues that are completely accessible. Values between 0.65 and 1 signify partial solvent access.

Tryptic mapping provides coverage for 10 of the 12 sulfur-containing residues in WaaL. F_u values of ~0.65 were observed for M19, M291, and M316, revealing that these

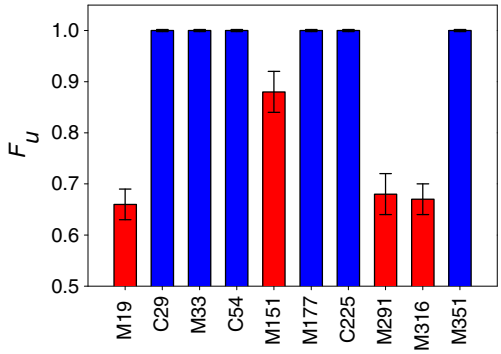

Figure 4. Oxidative labeling behavior of WaaL depicted for all Met and Cys residues that were covered by tryptic peptide mapping. Shown in this figure is the "fraction unmodified" (F_u) of potential oxidation sites (listed along the bottom) after hydroxyl radical exposure. Residues that undergo oxidation are indicated in red, while those that are not oxidizable are shown in blue. The color scheme used here mirrors that used in Figures 1 and 5

three residues are completely solvent-accessible (Figure 4). M151 shows an F_u value of 0.88, indicating that this residue is only partially solvent-accessible. Residues that undergo complete or partial labeling are highlighted in red (Figure 4). Complete protection with $F_u \approx 1$ is seen for C29, M33, C54, M177, C225, and M351 (blue in Figure 4), implying that these residues are not solvent accessible.

Topology Models and Oxidative Labeling Behavior

Comparison of the WaaL oxidative labeling data (Figure 4) with the predicted topology (Figure 1) [13] reveals that all six non-oxidized Cys and Met residues are in putative transmembrane helical regions. Three of the oxidized Met side chains, all with F_u values of ~0.65, are situated in regions that are predicted to be solvent-accessible. Specifically, M19 is located at the cytoplasmic membrane surface, and M291/M316 are positioned in the extramembrane domain EL5. The behavior of these nine residues is consistent with the topology model of Figure 1. However, the partial labeling of M151 is difficult to reconcile with the proposed position of this residue in transmembrane helix 5.

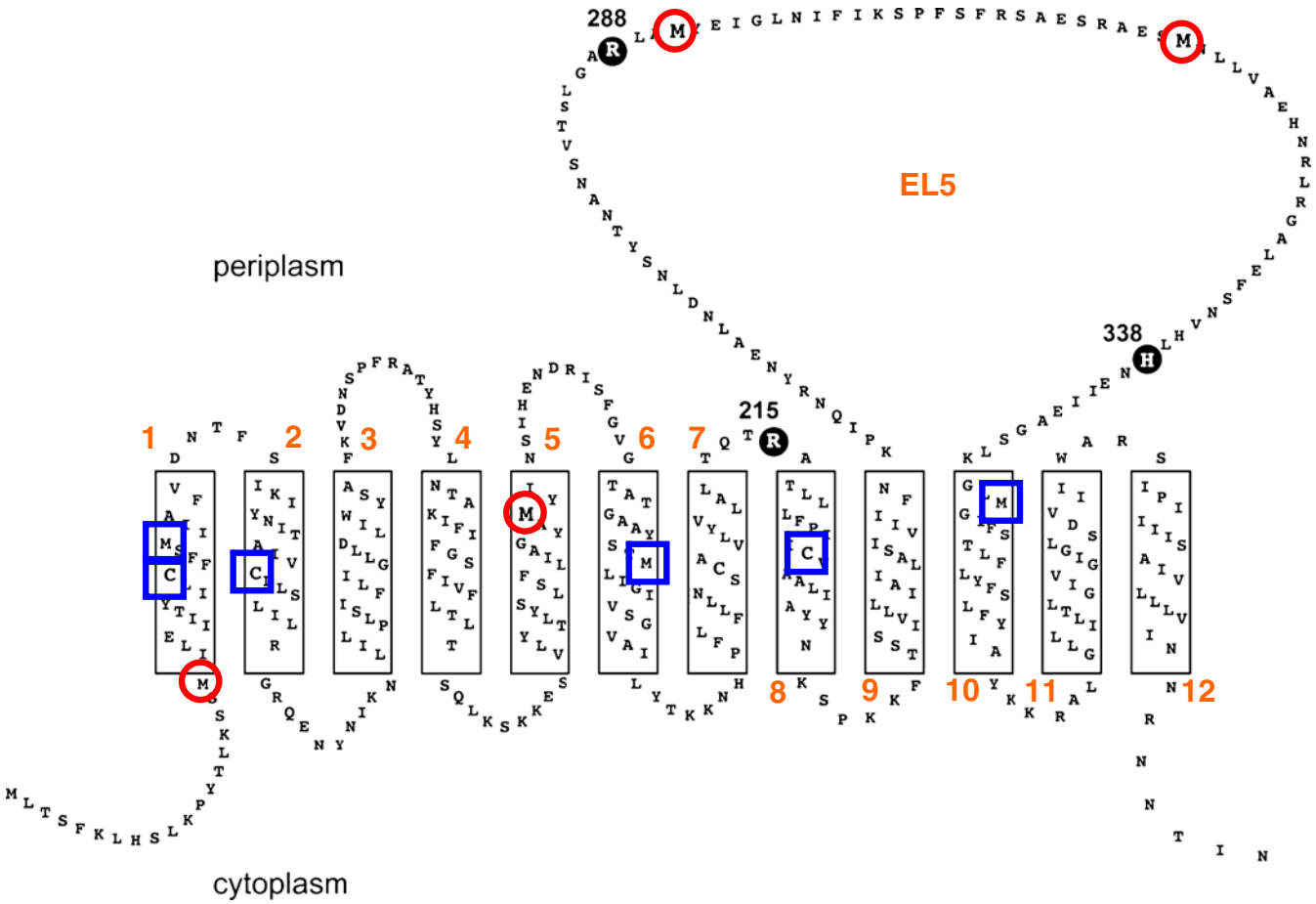

Figure 5. Modified WaaL topology model obtained using PolyPhobious [9]. The notation used is identical to that of Figure 1. Red circles indicate residues that undergo oxidative labeling. Non-oxidizable sites are highlighted by blue squares. As discussed in the text, this modified model is in better agreement with our oxidative labeling data than the original model of Figure 1

Other side chains that are predicted to occupy buried locations at a similar depth (e.g., M33 in helix 1) are completely protected from oxidation. Partial oxidation of M151, therefore, points to some inaccuracies of the originally proposed topology (Figure 1) [13].

The model of Figure 1 had been developed in 2008 [13] using the topology prediction routine TMHMM [60] (http://www.cbs.dtu.dk/services/TMHMM/), which employs hydropathy analyses in combination with a hidden Markov model to distinguish transmembrane helices from extramembrane loops. TMHMM generally provides models that quite closely resemble the actual topology of IMPs [60]. PolyPhobious (http://phobius.sbc.su.se/poly.html) is a program that operates on similar principles, but it additionally incorporates global sequence alignment data. Thus, PolyPhobious provides improved model predictions as verified in tests on reference IMPs of known topology [9]. Not surprisingly, subjecting the WaaL sequence to PolyPhobious results in a somewhat modified topology model (Figure 5).

The overall features of the initial WaaL model (Figure 1) [13] and the modified version (Figure 5) are very similar. Both models predict 12 transmembrane helices, with a large periplasmic EL5 domain. Close comparison, however, reveals some differences in the boundaries of transmembrane helices relative to their connecting extramembrane loops. Importantly, M151 in helix 5 is located closer to the periplasmic membrane surface in the modified model (position 3 in helix 5 [Figure 5], versus position 6 [Figure 1]). This modified position is in better agreement with the oxidation behavior of M151 (Figure 4). In particular, the observation of partial labeling (F_u=0.88) for M151 is consistent with the topology description of Figure 5 where this residue is placed close to the membrane interface, but not in full contact with the aqueous periplasmic space. One can contrast this behavior with that of M19, which is predicted to be directly at the interface (helix 1, Figure 5), consistent with its more extensive oxidation (F_u=0.66, Figure 4).

M351 represents another residue that has been placed closer to the periplasmic surface in the revised model (helix 10, Figure 5). Interestingly, this residue is inaccessible (F_u≈1, Figure 4). This labeling behavior of M351 is consistent with molecular dynamics simulations that predict a tightly folded globular structure for the extramembrane domain EL5 [13]. Helices 9 and 10 form the "stem" of EL5. Our results strongly suggest that this globular domain is packed tightly against the periplasmic interface of WaaL, thereby shielding the terminus of helix 10 (including M351) from solvent access in a lid-like fashion. The oxidation behavior of M151 indicates that this shielding does not extend to helix 5.

Overall, our laser-induced oxidative labeling experiments provide information on the solvent-accessibility of 10 highly reactive residues (Cys and Met) in WaaL. These data were used to test the accuracy of computer-generated topology maps. Most features of the measured protection pattern (Figure 4) are consistent with the initially developed model (Figure 1) [13]. However, the agreement between experiment and model can be further improved by employing the more comprehensive PolyPhobious algorithm that yields a slightly revised topology (Figure 5). Notably, the revised topology remains consistent with all of the mutational assays and fusion protein data that had originally been used to support the model of Figure 1 [13].

Conclusions

Computer-generated topology maps are widely used for low-resolution IMP structure predictions. In the absence of experimental data to support the resulting models, however, the value of such predictions remains questionable [10]. It is common practice to use various biochemical and mutational assays for the validation of computer-generated topology models [6, 10–16]. Those experimental techniques, however, are labor intensive and may induce structural artifacts.

The current work highlights an approach that can complement (or even replace) some of those traditional validation tools. We demonstrate that laser-induced oxidative labeling is suitable for rapidly testing computer-generated topology predictions. The experiments are based on the premise that differential protection of extramembrane regions and transmembrane helices will be reflected in the ·OH labeling levels. In cases where different software algorithms provide diverging models, oxidative labeling offers a stringent selection tool. Indeed, we demonstrate that it is possible to differentiate residues that exhibit different degrees of labeling, ranging from completely buried in the bilayer, to partially buried at the membrane interface, to fully solvent-accessible.

We anticipate the possibility to include oxidative labeling data as a priori constraints in future topology prediction programs. Such an approach may be preferable to the use of oxidative labeling data for the post-processing assessment of competing models. The mutational introduction of additional easily oxidizable residues in strategic locations will further enhance the resolution of the approach used here [61]. In addition, it may be possible to conduct labeling experiments on IMPs in their natural bilayer environment (possibly even in vivo), instead of relying on purified proteins. Encouraging initial steps in this direction have recently been reported [34, 54].

Acknowledgments

The authors acknowledge support for this work by grants from the Natural Sciences and Engineering Research Council of Canada, and the Canadian Institutes of Health Research. M.A.V. and L.K. hold Canada Research Chairs.

References

1. Wu, C.C., Yates III, J.R.: The application of mass spectrometry to membrane proteins. *Nat. Biotechnol.* **21**, 262–267 (2003)
2. George, S.R., O'Dowd, B.F., Lee, S.P.: G-Protein-Coupled Receptor Oligomerization and its Potential for Drug Discovery. *Nat. Rev. Drug Discov.* **1**, 808–820 (2002)
3. White, S.H.: Biophysical dissection of membrane proteins. *Nature* **459**, 344–346 (2009)

4. Barth, P., Wallner, B., Baker, D.: Prediction of membrane protein structures with complex topologies using limited constraints. *Proc. Natl. Acad. Sci. U.S.A.* **106**, 1409–1414 (2009)
5. Garavito, R.M., Ferguson-Miller, S.: Detergents as Tools in Membrane Biochemistry. *J. Biol. Chem.* **276**, 32403–32406 (2001)
6. Drew, D., Sjöstrand, D., Nilsson, J., Urbig, T., Chin, C.N., de Gier, J. W., von Heijne, G.: Rapid topology mapping of Escherichia coli inner-membrane proteins by prediction and PhoA/GFP fusion analysis. *Proc. Natl. Acad. Sci. U.S.A.* **99**, 2690–2695 (2002)
7. Kyte, J., Doolittle, R.: A simple method for displaying the hydropathic character of a protein. *J. Mol. Biol.* **157**, 105–132 (1982)
8. Tusnády, G.E., Simon, I.: The HMMTOP transmembrane topology prediction server. *Bioinformatics* **17**, 849–850 (2001)
9. Käll, L., Krogh, A., Sonnhammer, E.L.: An HMM posterior decoder for sequence feature prediction that includes homology information. *Bioinformatics* **21**, i251–i257 (2005)
10. Bogdanov, M., Zhang, W., Xie, J., Dowhan, W.: Transmembrane protein topology mapping by the substituted cysteine accessibility method (SCAM^{TM}): Application to lipid-specific membrane protein topogenesis. *Methods* **36**, 148–171 (2005)
11. Frillingos, S., Sahin-Tótha, M., Wua, J., Kaback, H.R.: Cys-scanning mutagenesis: a novel approach to structure–function relationships in polytopic membrane proteins. *FASEB J.* **12**, 1281–1299 (1998)
12. Lorenz, H., Hailey, D.W., Wunder, C., Lippincott-Schwartz, J.: The fluorescence protease protection (FPP) assay to determine protein localization and membrane topology. *Nat. Protoc.* **1**, 276–279 (2006)
13. Pérez, J.M., McGarry, M.A., Marolda, C.L., Valvano, M.A.: Functional analysis of the large periplasmic loop of the Escherichia coli K-12 WaaL O-antigen ligase. *Mol. Microbiol.* **70**, 1424–1440 (2008)
14. Alexeyev, M.F., Winkler, H.H.: Membrane topology of the Rickettsia prowazekii ATP/ADP translocase revealed by novel dual pho-lac reporters. *J. Mol. Biol.* **285**, 1503–1513 (1999)
15. Islam, S.T., Taylor, V.L., Qi, M., Lam, J.S.: Membrane topology mapping of the O-antigen flippase (Wzx), polymerase (Wzy), and ligase (WaaL) from Pseudomonas aeruginosa PAO1 reveals novel domain architectures. *MBio.* **1**, 1–10 (2010)
16. Feilmeier, B.J., Iseminger, G., Schroeder, D., Webber, H., Phillips, G.J.: Green fluorescent protein functions as a reporter for protein localization in *Escherichia coli*. *J. Bacteriol.* **182**, 4068–4076 (2000)
17. Carroll, J., Fearnley, I.M., Walker, J.E.: Definition of the mitochondrial proteome by measurements of molecular masses of membrane proteins. *Proc. Natl. Acad. Sci. U.S.A.* **103**, 16170–16175 (2006)
18. Weiner, J.H., Li, L.: Proteome of the *Escherichia coli* envelope and technological challenges in membrane proteome analysis. *Biochim. Biophys. Acta* **1778**, 1698–1713 (2008)
19. Whitelegge, J.P., Halgand, F., Souda, P., Zabrouskov, V.: Top-down Mass Spectrometry of Integral Membrane Proteins. *Exp. Rev. Proteomics* **3**, 585–596 (2006)
20. Barrera, N.P., Robinson, C.V.: Advances in the Mass Spectrometry of Membrane Proteins: From Individual Proteins to Intact Complexes. *Annu. Rev. Biochem.* **80**, 247–271 (2011)
21. Busenlehner, L.S., Salomonsson, L., Brzezinski, P., Armstrong, R.N.: Mapping protein dynamics in catalytic intermediates of the redox-driven proton pump cytochrome *c* oxidase. *Proc. Natl. Acad. Sci. U.S.A.* **103**, 15398–15403 (2006)
22. Joh, N.H., Min, A., Faham, S., Whitelegge, J.P., Yang, D., Woods, V. L., Bowie, J.U.: Modest stabilization by most hydrogen-bonded side-chain interactions in membrane proteins. *Nature* **453**, 1266–1270 (2008)
23. Zhang, X., Chien, E.Y.T., Chalmers, M.J., Pascal, B.D., Gatchalian, J., Stevens, R.C., Griffin, P.R.: Dynamics of the b2-Adrenergic G-Protein Coupled Receptor Revealed by Hydrogen–Deuterium Exchange. *Anal. Chem.* **82**, 1100–1108 (2010)
24. Hebling, C.M., Morgan, C.R., Stafford, D.W., Jorgenson, J.W., Rand, K.D., Engen, J.R.: Conformational Analysis of Membrane Proteins in Phospholipid Bilayer Nanodiscs by Hydrogen Exchange Mass Spectrometry. *Anal. Chem.* **82**, 5415–5419 (2010)
25. Rey, M., Man, P., Clémençon, B., Trézéguet, V., Brandolin, G., Forest, E., Pelosi, L.: Conformational dynamics of the bovine mitochondrial ADP/ATP carrier isoform 1 revealed by hydrogen/deuterium exchange coupled to mass spectrometry. *J. Biol. Chem.* **285**, 34981–34990 (2010)
26. West, G.M., Chien, E.Y.T., Katritch, V., Gatchalian, J, Chalmers, M.J., Stevens, R.C., Griffin, P.R.: Ligand-Dependent Perturbation of the Conformational Ensemble for the GPCR b2 Adrenergic Receptor Revealed by HDX. *Structure* **19,** 1424–1432 (2011).
27. Stelzer, W., Poschner, B.C., Stalz, H., Heck, A.J., Langosch, D.: Sequence-specific conformational flexibility of SNARE transmembrane helices probed by hydrogen/deuterium exchange. *Biophys. J.* **95**, 1326–1335 (2008)
28. Trimpin, S., Brizzard, B.: Analysis of Insoluble Proteins. *Biotechniques* **46**, 409–419 (2009)
29. Mendoza, V.L., Vachet, R.W.: Probing Protein Structure by Amino Acid-specific Covalent Labeling and Mass Spectrometry. *Mass Spectrom. Rev.* **28**, 785–815 (2009)
30. Fitzgerald, M.C., West, G.M.: Painting Proteins with Covalent Labels: What's In the Picture? *J. Am. Soc. Mass Spectrom.* **20**, 1193–1206 (2009)
31. Xu, G., Chance, M.R.: Hydroxyl Radical-Mediated Modification of Proteins as Probes for Structural Proteomics. *Chem. Rev.* **107**, 3514–3543 (2007)
32. Pan, Y., Konermann, L.: Membrane protein structural insights from chemical labeling and mass spectrometry. *Analyst* **135**, 1191–1200 (2010)
33. Li, C., Takazaki, S., Jin, X., Kang, D., Abe, H., Hamasaki, N.: Identification of Oxidized Methionine Sites in Erythrocyte Membrane Protein by Liquid Chromatography/Electrospray Ionization Mass Spectrometry Peptide Mapping. *Biochemistry* **45**, 12117–12124 (2006)
34. Zhu, Y., Guo, T., Park, J.-H., Li, X., Meng, W., Datta, A., Bern, M., Lim, S.K., Sze, S.K.: Elucidating in vivo structural dynamics in integral membrane protein by hydroxyl radical footprinting. *Mol. Cell. Proteomics* **8**, 1999–2010 (2009)
35. Smedley, J.G., Sharp, J.S., Kuhn, J.F., Tomer, K.B.: Probing the pH-dependent prepore to pore transition of Bacillus anthracis protective antigen with differential oxidative protein footprinting. *Biochemistry* **47**, 10694–10704 (2008)
36. Orban, T., Gupta, S., Palczewski, K., Chance, M.R.: Visualizing Water Molecules in Transmembrane Proteins Using Radiolytic Labeling Methods. *Biochemistry* **49**, 827–834 (2010)
37. Weinglass, A.B.: Probing the Structure and Function of Integral Membrane Proteins by Mass Spectrometry. In: Whitelegge, J.P. (ed.) Protein Mass Spectrometry, vol. 52, pp. 197–212. Elsevier, Amsterdam (2009)
38. Leite, J.F., Blanton, M.P., Shahgholi, M., Dougherty, D.A., Lester, H. A.: Conformation-dependent hydrophobic photolabeling of the nicotinic receptor: Electrophysiology-coordinated photochemistry and mass spectrometry. *Proc. Natl. Acad. Sci. U.S.A.* **100**, 13054–13059 (2003)
39. Wen, J., Zhang, H., Gross, M.L., Blankenship, R.E.: Membrane Orientation of the FMO Antenna Protein from *Chlorobaculum tepidum* as Determined by Mass Spectrometry-based Footprinting. *Proc. Natl. Acad. Sci. U.S.A.* **106**, 6134–6139 (2009)
40. Weinglass, A.B., Whitelegge, J.P., Hu, Y., Verner, G.E., Faull, K.F., Kaback, H.R.: Elucidation of substrate binding interactions in a membrane transport protein by mass spectrometry. *EMBO J.* **22**, 1467–1477 (2003)
41. Kelly, B.L., Gross, A.: Potassium channel Gating Observed with Site-directed Mass Tagging. *Nat. Struct. Biol.* **10**, 280–284 (2003)
42. Pan, Y., Brown, L., Konermann, L.: Kinetic Folding Mechanism of an Integral Membrane Protein Examined by Pulsed Oxidative Labeling and Mass Spectrometry. *J. Mol. Biol.* **410**, 146–158 (2011)
43. McClintock, C., Kertesz, V., Hettich, R.L.: Development of an Electrochemical Oxidation Method for Probing Higher Order Protein Structure with Mass Spectrometry. *Anal. Chem.* **80**, 3304–3317 (2008)
44. Sharp, J.S., Becker, J.M., Hettich, R.L.: Analysis of protein solvent accessible surfaces by photochemical oxidation and mass spectrometry. *Anal. Chem.* **76**, 672–683 (2004)
45. Maleknia, S.D., Downard, K.: Radical Approaches to Probe Protein Structure, Folding, and Interactions by Mass Spectrometry. *Mass Spectrom. Rev.* **20**, 388–401 (2001)
46. Watson, C., Janik, I., Zhuang, T., Charvatova, O., Woods, R.J., Sharp, J.S.: Pulsed Electron Beam Water Radiolysis for Submicrosecond Hydroxyl Radical Protein Footprinting. *Anal. Chem.* **81**, 2496–2505 (2009)
47. Nukuna, B.N., Sun, G., Anderson, V.E.: Hydroxyl Radical Oxidation of Cytochrome c by Aerobic Radiolysis. *Free Radical Biol. Med.* **37**, 1203–1213 (2004)
48. Hambly, D.M., Gross, M.L.: Laser Flash Photolysis of Hydrogen Peroxide to Oxidize Protein Solvent-Accessible Residues on the Microsecond Timescale. *J. Am. Soc. Mass Spectrom.* **16**, 2057–2063 (2005)

49. Konermann, L., Pan, Y., Stocks, B.B.: Protein folding mechanisms studied by pulsed oxidative labeling and mass spectrometry. *Curr. Opin. Struct. Biol.* **21**, 634–640 (2011)
50. Gau, B.C., Sharp, J.S., Rempel, D.L., Gross, M.L.: Fast Photochemical Oxidation of Protein Footprints Faster than Protein Unfolding. *Anal. Chem.* **81**, 6563–6571 (2009)
51. Konermann, L., Stocks, B.B., Czarny, T.: Laminar Flow Effects During Laser-Induced Oxidative Labeling For Protein Structural Studies by Mass Spectrometry. *Anal. Chem.* **82**, 6667–6674 (2010)
52. Konermann, L., Tong, X., Pan, Y.: Protein Structure and Dynamics Studied by Mass Spectrometry: H/D exchange, hydroxyl radical labeling, and related approaches. *J. Mass Spectrom.* **43**, 1021–1036 (2008)
53. Wang, L., Chance, M.R.: Structural Mass Spectrometry of Proteins Using Hydroxyl Radical Based Protein Footprinting. *Anal. Chem.* **83**, 7234–7241 (2011)
54. Pan, Y., Stocks, B.B., Brown, L., Konermann, L.: Structural Characterization of an Integral Membrane Protein in its Natural Lipid Environment by Oxidative Methionine Labeling and Mass Spectrometry. *Anal. Chem.* **81**, 28–35 (2009)
55. Pan, Y., Piyadasa, H., O'Neil, J.D., Konermann, L. Conformational Dynamics of a Membrane Transport Protein Probed by H/D Exchange and Covalent Labeling: The Glycerol Facilitator. *J. Mol. Biol.* **2012,** *(in press)*, doi:10.1016/j.jmb.2011.12.052.
56. Nikaido, H.: Molecular basis of bacterial outer membrane permeability revisited. *Microbiol. Mol. Biol. Rev.* **67**, 593–656 (2003)
57. Valvano, M.A., Furlong, S.E., Patel, K.A.: Genetics, biosynthesis and assembly of O antigen. In: Knirel, Y., Valvano, M.A. (eds.) Bacterial lipopolysaccharides: Structure, chemical synthesis, biogenesis and interaction with host cells, pp. 275–310. Springer Verlag Publishing Inc, Weinheim (2011)
58. Valvano, M.A.: Common themes in glycoconjugate assembly using the biogenesis of O-antigen lipopolysaccharide as a model system. *Biochem. Mosc.* **76**, 729–735 (2011)
59. Ruan, X., Loyola, D.E., Marolda, C.L., Perez-Donoso, J.M., Valvano, M.A. The WaaL O-antigen lipopolysaccharide ligase has features in common with metal ion-independent inverting glycosyltransferases. *Glycobiology* **2011,** in press, doi: 10.1093/glycob/cwr150.
60. Sonnhammer, E.L.L., von Heijne, G., Krogh, A.: A hidden Markov model for predicting transmembrane helices in protein sequences. In: Glasgow, J., Littlejohn, T., Major, F., Lathrop, R., Sankoff, D., Sensen, C. (eds.) Proceedings of the Sixth International Conference on Intelligent Systems for Molecular Biology, pp. 175–182. AAAI Press, Menlo Park, CA (1998)
61. Pan, Y., Brown, L., Konermann, L.: Site-Directed Mutagenesis Combined with Oxidative Methionine Labeling for Probing Structural Transitions of a Membrane Protein by Mass Spectrometry. *J. Am. Soc. Mass Spectrom.* **21**, 1947–1956 (2010)
62. Hambly, D.M., Gross, M.L.: Cold Chemical Oxidation of Proteins. *Anal. Chem.* **81**, 7235–7242 (2009)
63. Xu, G., Kiselar, J., He, Q., Chance, M.R.: Secondary Reactions and Strategies To Improve Quantitative Protein Footprinting. *Anal. Chem.* **77**, 3029–3037 (2005)
64. Saladino, J., Liu, M., Live, D., Sharp, J.S.: Aliphatic Peptidyl Hydroperoxides as a Source of Secondary Oxidation in Hydroxyl Radical Protein Footprinting. *J. Am. Soc. Mass Spectrom.* **20**, 1123–1126 (2009)
65. Perdivara, I., Deterding, L.J., Przybylski, M., Tomer, K.B.: Mass Spectrometric Identification of Oxidative Modifications of Tryptophan Residues in Proteins: Chemical Artifact or Post-Translational Modification? *J. Am. Soc. Mass Spectrom.* **21**, 1114–1117 (2010)
66. Lin, W.J., Hwang, M.J.: VHMPT: A graphical viewer and editor for helical membrane protein topologies. *Bioinformatics* **14**, 866–868 (1998)